

Research Article

Effects of Pipe Roof Support and Grouting Pre-Reinforcement on the Track Settlement

Kui Wu and Zhushan Shao 

School of Civil Engineering, Xi'an University of Architecture & Technology, Xi'an 710055, China

Correspondence should be addressed to Zhushan Shao; shaozhushan@xauat.edu.cn

Received 22 September 2018; Revised 6 November 2018; Accepted 26 November 2018; Published 26 December 2018

Academic Editor: Hossein Moayedi

Copyright © 2018 Kui Wu and Zhushan Shao. This is an open access article distributed under the Creative Commons Attribution License, which permits unrestricted use, distribution, and reproduction in any medium, provided the original work is properly cited.

Based on the first shallow tunnel passing below an active railway station in the loess area in China, studies on the tunnel deformation and track settlement during tunneling are performed by using FLAC3D. It is found that, without adopting other reinforcement measures, the maximum track settlement has far exceeded engineering requirements. To reduce deformations induced by the tunneling, the combined presupport technique of the pipe roof and grouting reinforcement is presented and optimal construction parameters are provided. It is concluded that the installation of the pipe roof support plays an important role in controlling tunnel crown settlement and track settlement. The optimal pipe diameter is 159 mm, and the optimal arrangement area of the pipe roof is 150°. Grouting could improve soil strength and reduce deformations. The optimal thickness of the grouting reinforcement ring is 2 m. When the optimal parameters of the combined presupport technique are adopted, calculation results show that the maximum track settlement would reach 13.8 mm, which realized the settlement control goal of a maximum value of 15 mm. At last, the combined presupport technique proposed has been well validated in the “Railway Station” of Metro Line 4.

1. Introduction

In the past few decades, increasing demands on infrastructures increase attention on shallow soft ground tunneling methods in many urbanized areas. Many surface and subsurface structures make underground excavation works very delicate to the influence of deformation, which should be definitely limited to tolerable values [1]. The influence of underground construction on surface and subsurface structures should be accurately predicted, and corresponding remedial measures have to be put forward and taken prior to excavation.

Many efforts have been contributed to minimizing the negative effect due to underground construction [2–11]. Hasanpour et al. [12] investigated the effects of pipe roofing on surface settlements and evaluated the settlements associated with the twin tunnels in the Istanbul Metro by using numerical, semiempirical, and measured values. Yu et al. [13] evaluated the influence of blasting vibrations on the tunnel in soft soils in the city of Shanghai. Liu et al. [14]

suggested to use the pile-beam-arch method to control the surface settlement induced by metro tunnel excavation. Sadaghiani and Dadizadeh [15] introduced the concrete-arch presupporting system in the metro underground station in Tabriz, Iran. Kivi et al. [16] carried out a numerical analysis on surface settlement using the central beam column structure. For tunneling in the loess area, Zhao et al. [17] systematically summarized the technical characteristics and main problems of the large-section loess tunnels in China's speed railway, including classification of the surrounding rock, design of the supporting structure, surface settlement and cracking control, and safe and rapid construction methods. Li et al. [18] discussed the effects of the three-bench seven-step excavation method (TSEM) on the displacement characteristics for high-speed railway (HSR) tunnels. Qiu et al. [19] investigated the response of the metro tunnel under the local dynamic water environment. However, the above research studies have not involved the influence of tunneling on track settlement in the loess area and not provided effective solutions as well.

Based on the first shallow tunnel passing below an active railway station in the loess area in China, this paper deals with tunnel deformation and track settlement during tunneling by using FLAC3D. In order to meet engineering requirements, the combined pre-reinforcement technique is presented and optimal supporting parameters are further investigated. This paper could provide useful guidance for similar projects.

2. Engineering Background and Numerical Model

2.1. Background. “Railway Station” of Xi'an Metro Line 4 is the first shallow metro tunnel with a large cross section passing below an active railway station in the loess area in China, which is the critical project of Metro Line 4. Layout of “Railway Station” of Metro Line 4 is shown in Figure 1(a). The center cross diagram (CRD) method is used in the construction of this metro tunnel. During tunneling, many rail tracks would be affected, including ten single tracks, four single turnouts, and one double turnout, which is the first case throughout the world. Strict track settlement control of a maximum value of 15 mm is asked.

Complicated geological conditions of the construction site also challenge tunneling. The soil profile for the construction site mainly consists of saturated soft loess, silty clay, new loess, and plain filling soil, as illustrated in Figure 1(b). Specially, saturated soft loess presents soft-plastic property and local plastic flow with high compressibility. Attention needs be paid to minimize the disturbance of the saturated soft loess layer during tunneling.

2.2. Numerical Model and Parameters. To minimize the boundary effects on numerical results, the model size is adopted over three times the tunnel size, and the length, width, and height of the model are 170 m, 100 m, and 85 m, respectively, as shown in Figure 2. The tunnel central axis is parallel with model width and perpendicular to length. In regard to six surfaces of the 3D model, only the top surface is free, while other five surfaces are completely constrained. Three rail tracks on-site are selected and modeled to investigate the rule of track settlement induced by tunneling. Meanwhile, seven monitoring points are arranged in each rail track in Figure 2. Other details about the model are given in Figure 2.

The Mohr–Coulomb elastic-plastic constitutive model is selected to describe deformation behavior of soil mass, and rail tracks, subgrade, track bed, and lining are all assumed to be elastic in the model. In FLAC3D, rail tracks are simulated by the beam element, and based on the solid element, track bed and soil mass are modeled. Only geostatic stress is accounted for in this shallow tunnel model. Computing parameters are listed in Table 1.

2.3. Model Verification. As shown in Figures 3(a) and 3(b), curves for crown settlement of the monitored cross section with its distance from the tunnel face and track settlement of monitored points are plotted, respectively. The good agreement of the numerical results with the

monitored data demonstrates the rationality and effectiveness of the numerical model. From Figure 3(b), it can be observed that the maximum track settlement has far exceeded 15 mm, and thus, it is pretty necessary to take remedial measures.

3. Pipe Roof Support

The pipe roof support technique has been widely applied as one of the important auxiliary methods for shallow tunnel excavation. The pipe roof support can consolidate the ground stress and disperse the ground stress and reduce the excavation release stress, which effectively limits the tunnel crown settlement or prevent ground settlement.

3.1. Selection of Pipe Type. Currently, steel pipes with a diameter between 89 mm and 186 mm are more applied in practical engineering. Modulus and density of the steel pipe are 210 GPa and 2700 kg/m³, respectively, with those of the grouting material being 23 GPa and 2200 kg/m³, respectively. In the following numerical analysis, six types of pipes are simulated to investigate the effect of pipe parameters (R : diameter; s : thickness; S_g : effective area of concrete; S_c : effective area of the steel pipe; I_1 : moment of inertia of the steel pipe; I_2 : moment of inertia of concrete; E : elastic modulus of the grouting steel pipe; and ρ : density of the grouting pipe) on deformation, and their computing parameters are shown in Table 2. It is worth noting that the pipe roof supports all range from 0° to 90°.

Tunnel deformation and maximum track settlement using different types of pipes are provided in Table 3. Comparing with the results in Figure 3, it could be found that the installation of the pipe roof plays an important role in controlling deformation. Stiffness of the grouting pipe has a close relationship with pipe diameter. The grouting pipe with a larger diameter possesses greater stiffness, which means stronger antideforming capability. In the shallow tunnel, it is indicated that vertical pressure acting on the lining is far more than horizontal pressure and crown settlement is the main form of tunnel deformation. Therefore, based on the results in Table 3, it could be explained that crown settlement is more sensitive to pipe parameter changes, but peripheral convergence is not.

Track settlement is greatly affected by crown settlement. From Table 3, it can be seen that when pipe diameter reaches 159 mm, the fall in both crown settlement and track settlement is not obvious with increasing pipe diameter. Thus, Scheme 4(d) could be considered to be optimal for this project.

3.2. Determination of Arrangement Area. Arrangement area of the pipe roof is one of the important construction parameters. In this study, in order to obtain the optimal arrangement area, four schemes are designed and shown in Figure 4.

From Table 4, it can be seen that the arrangement area of the pipe roof also has an impact on deformations. With increasing area, deformations all exhibit a decreasing trend.

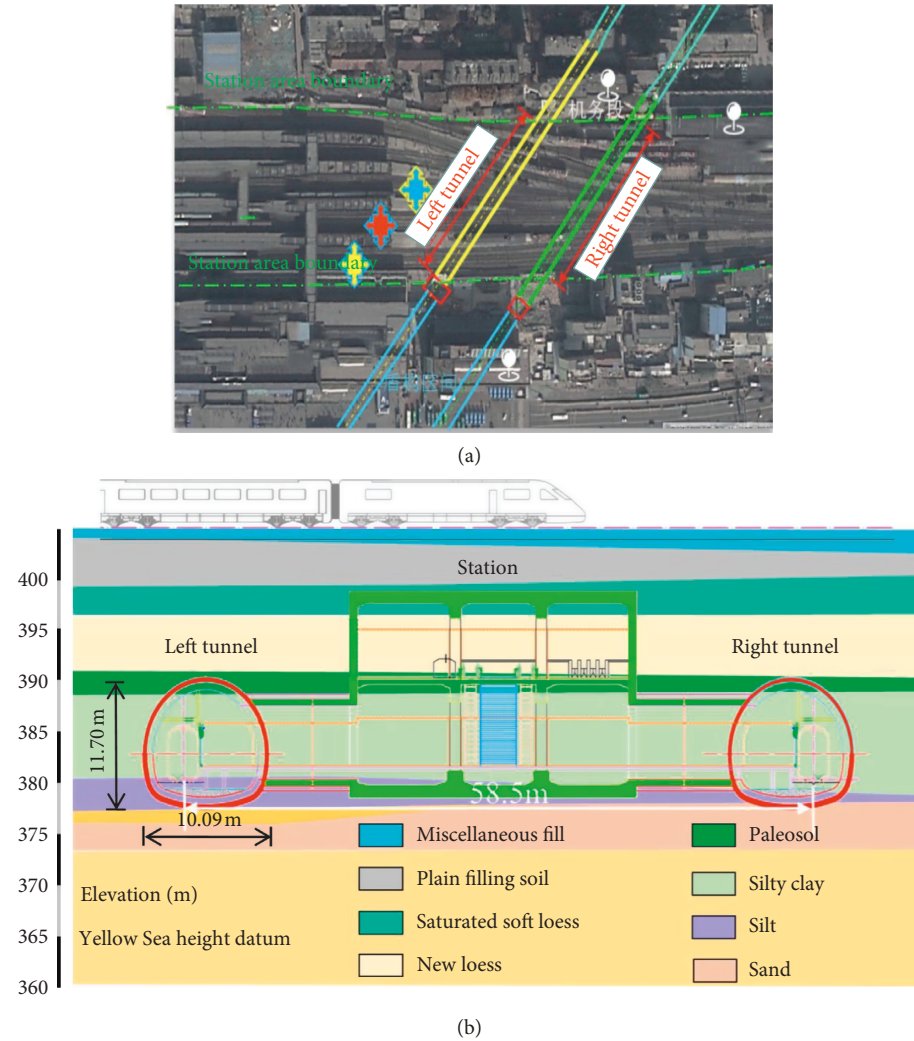


FIGURE 1: (a) Layout and (b) geology of “Railway Station” of Metro Line 4.

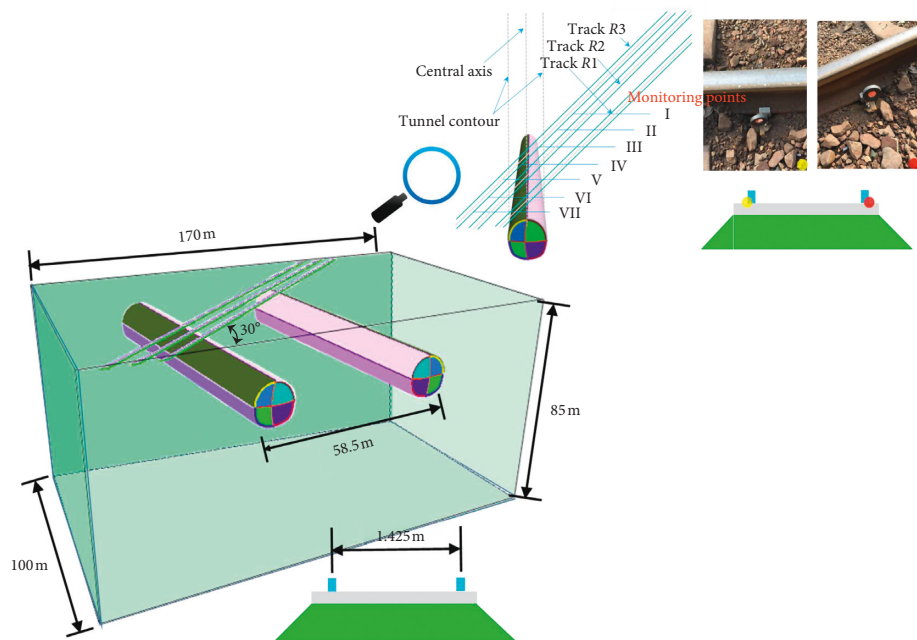


FIGURE 2: Illustration of the numerical model.

TABLE 1: Calculation parameters [20].

Material	Thickness (m)	Density (kg/m^3)	Elasticity modulus (MPa)	Poisson's ratio	Cohesion (kPa)	Internal friction angle ($^\circ$)
Miscellaneous soil	2.04	1600	9	0.41	5	6
Plain filling soil	2.56	1800	12	0.38	16	16
New loess (above the water level)	3.75	1800	15	0.34	34	20
Saturated soft loess	4.83	1750	8	0.32	38.2	19.5
New loess (under the water level)	3.09	1900	22	0.31	40	20.5
Paleosol	10.96	2010	33	0.30	48	21.5
Silty clay	57.78	2100	40	0.23	100	35
Track	0.07	2800	21	0.2	—	—
Track bed	0.15	2400	19	0.3	—	—
Subgrade	0.35	2800	19	0.24	—	—
Primary lining	0.3	2300	2000	0.26	—	—
Secondary lining	0.5	2500	2700	0.2	—	—

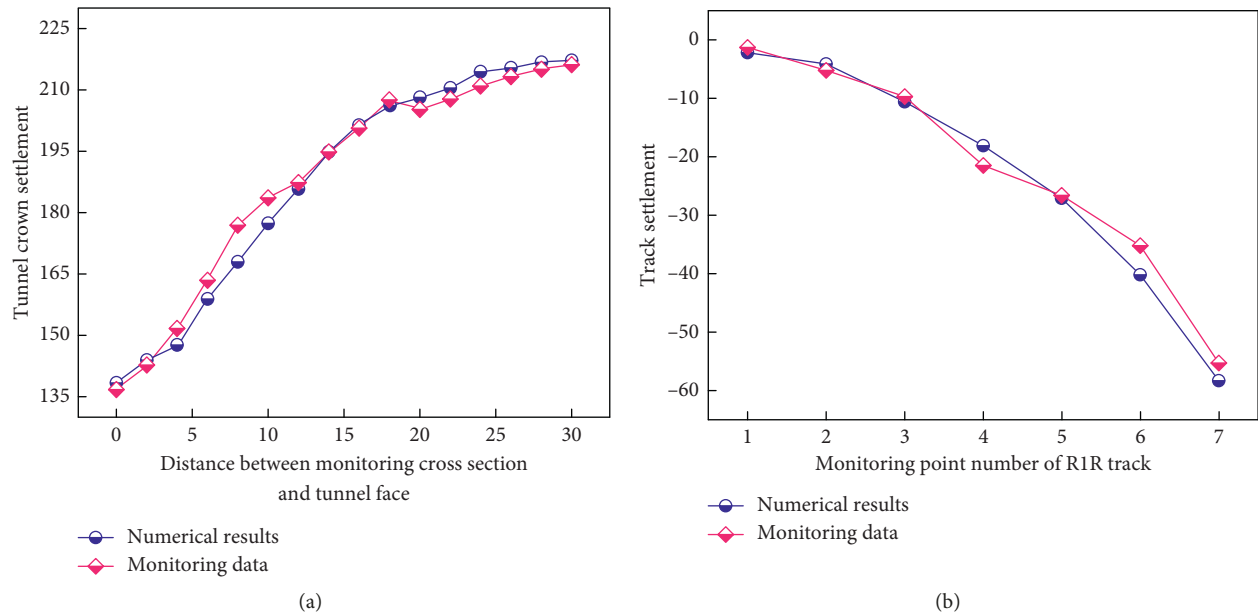


FIGURE 3: Comparison between numerical results and in situ data. (a) Tunnel crown settlement. (b) Track settlement.

TABLE 2: Cross section parameters of the grouting steel pipe.

Number	R (mm)	s (mm)	S_g (m^2)	S_c (m^2)	I_1 (m^4)	I_2 (m^4)	E (GPa)	ρ (kg/m^3)	Sketch
1	89	5	$2.35e^{-2}$	$2.72e^{-3}$	$6.36e^{-7}$	$1.49e^{-8}$	27.29	2371.25	
2	108	6	$3.46e^{-2}$	$3.96e^{-3}$	$1.36e^{-6}$	$7.04e^{-8}$	32.17	2369.44	
3	127	8	$4.75e^{-2}$	$6.18e^{-3}$	$2.90e^{-6}$	$2.49e^{-7}$	37.69	2390.86	
4	159	8	$7.54e^{-2}$	$7.79e^{-3}$	$5.85e^{-6}$	$1.59e^{-6}$	62.92	2354.17	
5	178	9	$9.45e^{-2}$	$9.81e^{-3}$	$9.24e^{-6}$	$3.92e^{-6}$	78.68	2354.90	
6	186	10	$1.03e^{-1}$	$1.14e^{-2}$	$1.17e^{-5}$	$5.49e^{-6}$	82.90	2364.24	

TABLE 3: Deformations using different types of pipes.

Number	Crown settlement (mm)	Peripheral convergence (mm)	Maximum track settlement (mm)
1	149.2	15.2	44.7
2	124.4	14.4	38.1
3	108.0	13.1	33.2
4	93.2	12.2	30.4
5	88.3	11.9	29.5
6	86.9	10.6	29.0

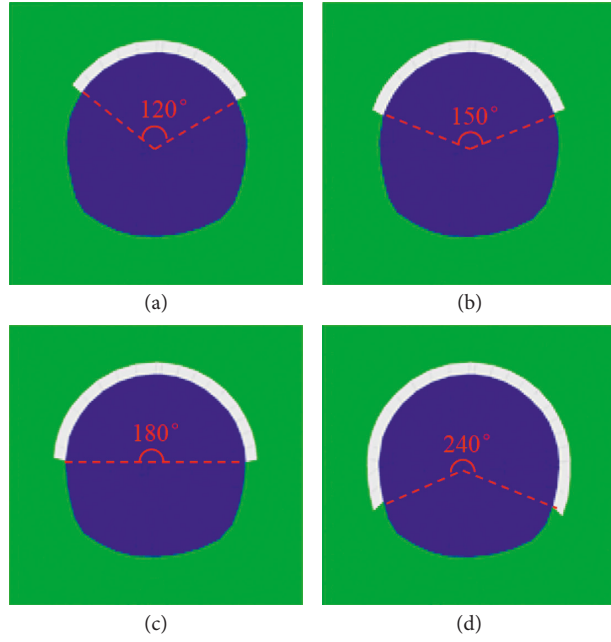


FIGURE 4: Arrangement area of the pipe roof.

TABLE 4: Deformations with different arrangement areas of the pipe roof.

Number	Crown settlement (mm)	Peripheral convergence (mm)	Maximum track settlement (mm)
1	85.3	11.3	26.6
2	80.9	3.2	23.4
3	78.2	2.9	22.5
4	73.3	2.7	22.0

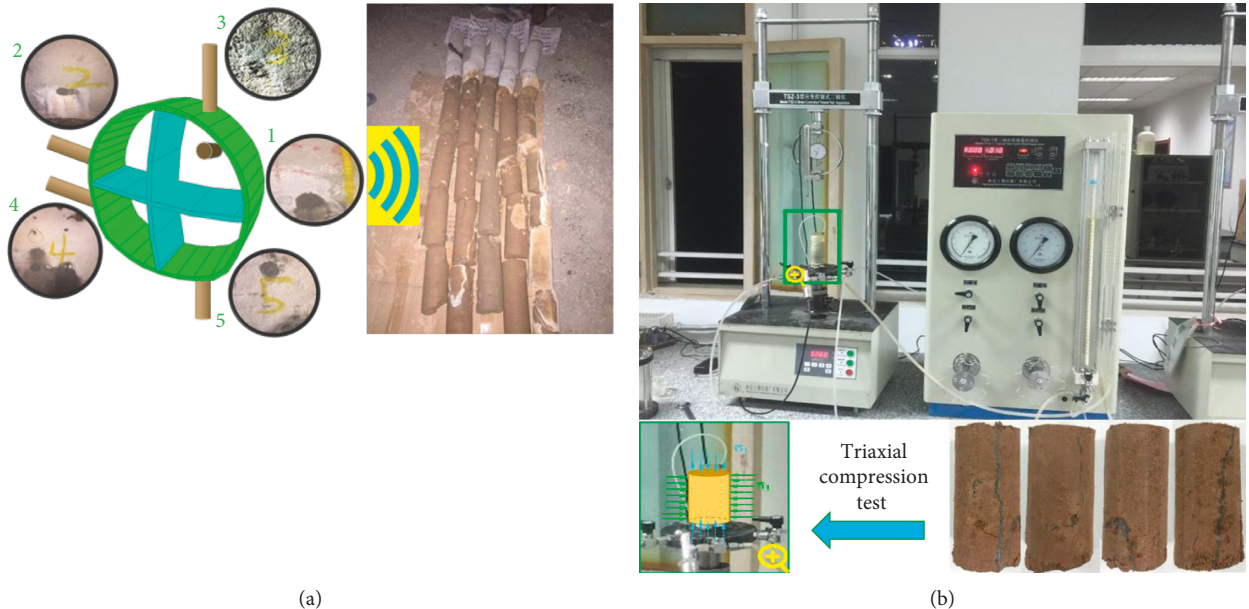


FIGURE 5: (a) Sampling in situ. (b) Laboratory test.

Maximum track settlement drops quickly when area ranges from 120° to 150°. Specially, peripheral convergence declines sharply from 11.3 mm to 3.2 mm, and afterwards, there is no distinct reduction with pipe roof area reaching 150°. So 150°

should be adopted as the optimal parameter for the pipe roof area. In such a case, requirements for maximum track settlement still could not be satisfied and other control measures need to be taken.

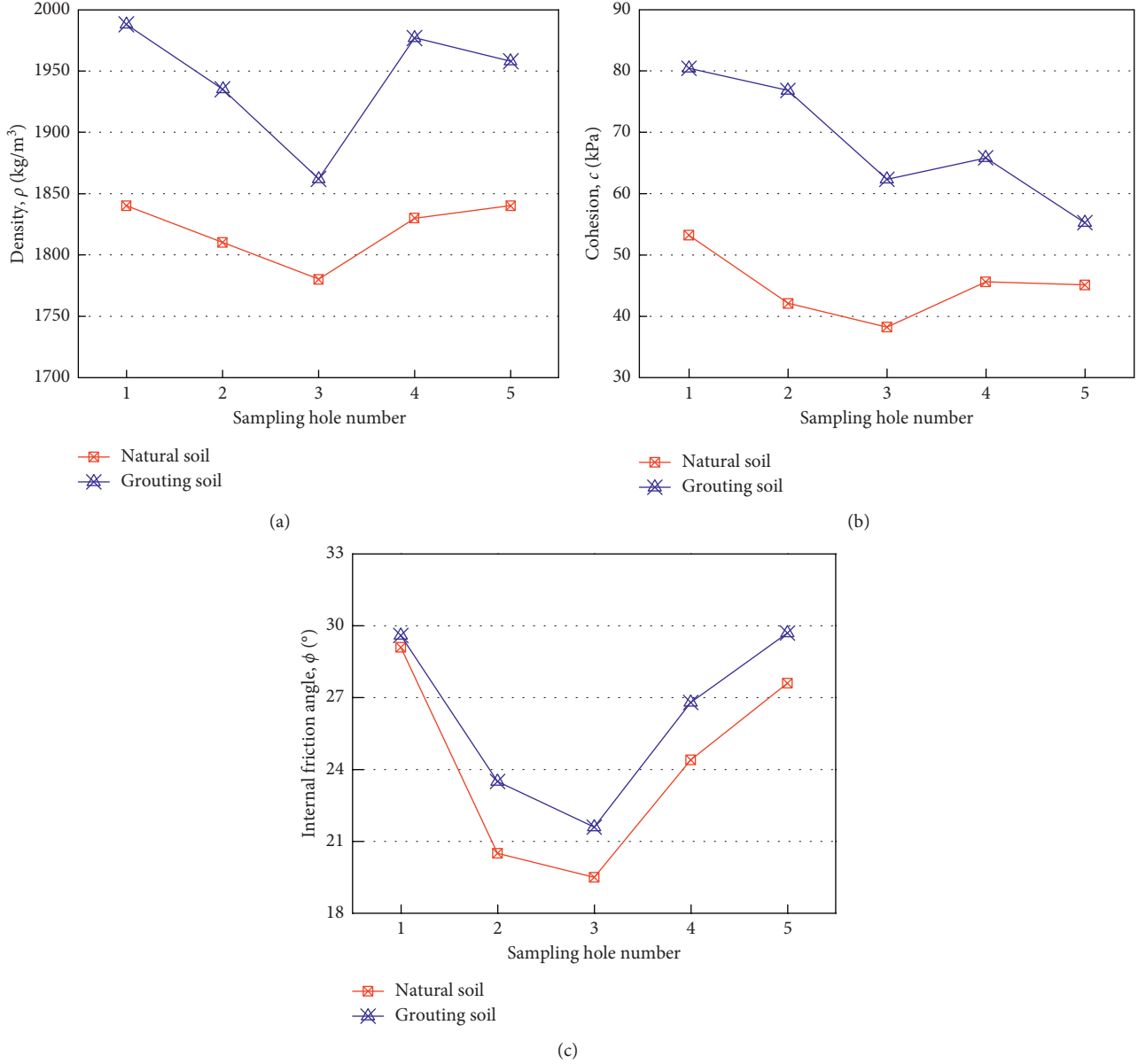


FIGURE 6: Comparison of (a) density, (b) cohesion, and (c) internal friction angle between natural and grouting soil.

4. Grouting Pre-Reinforcement

In the loess area, grouting pre-reinforcement is an ideal measure for reducing tunnel deformation during underground excavation. Studies show grouting pre-reinforcement could significantly improve performance of bearing capacity of soft surrounding rock and form a reinforcement ring around the tunnel. Thus, the stress state of the lining could be adjusted and tunnel stability enhanced. In this section, the effect of grouting pre-reinforcement on deformations is investigated.

4.1. Physical and Mechanical Properties of Grouting Soil

In the construction site, five sampling points are determined and displayed in Figure 5(a). In order to obtain soil parameters after grouting, experiments for density, cohesion,

TABLE 5: Basic parameters of grouting soil.

Number	Density ρ (kg/m^3)	Cohesion c (kPa)	Internal friction angle φ (°)
1	1988	80.4	29.6
2	1935	76.8	23.5
3	1862	62.3	21.6
4	1977	65.8	26.8
5	1958	55.2	29.7
Average	1944	68.1	26.2

and internal friction angle are carried out, as shown in Figure 5(b). Test results are shown in Figures 6(a)–6(c), respectively.

Figures 6(a) and 6(b) show that both density and cohesion c of soil obviously increase after grouting. By comparison, internal friction angle φ increases slightly in

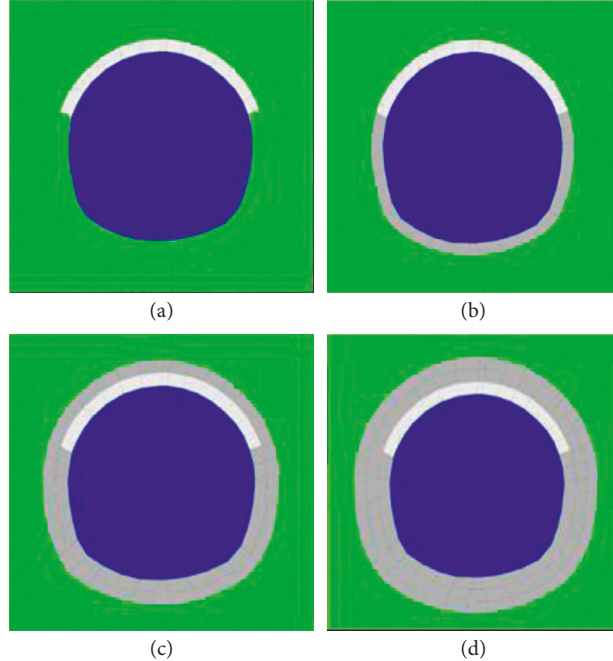


FIGURE 7: Reinforcement schemes of soil. (a) GP-0. (b) GP-1. (c) GP-2. (d) GP-3.

Figure 6(c). The average of each parameter after grouting is calculated and determined to be a simulation parameter for the grouting reinforcement ring and listed in Table 5.

4.2. Determination of Thickness of Grouting Reinforcement Ring. In order to determine reasonable thickness of the grouting reinforcement ring, as shown in Figure 7, thicknesses of 1 m, 2 m, and 3 m are planned to be calculated in numerical analysis, respectively. Here, the scheme of GP-0 is displayed to facilitate discussion on the grouting pre-reinforcement effect.

As shown in Figure 8(a), the curve for volume of the plastic zone with different reinforcement ring thicknesses is plotted. It is clear that grouting pre-reinforcement could significantly reduce the volume of the plastic zone in surrounding soil. If grouting pre-reinforcement is not adopted, volume of the plastic zone would reach about 1133 m^3 , which is 1.5 times that in the condition of 1 m reinforcement thickness. By comparison, this downturn of volume of the plastic zone becomes more gentle with reinforcement thickness changing from 1 m to 3 m.

Figures 8(b) and 8(c) show the tunnel crown settlement and track settlement with different reinforcement ring thicknesses. Obviously, both crown settlement and track settlement are greatly affected by grouting pre-reinforcement. Remarkably, thickness of 2 m is a critical parameter for the grouting reinforcement ring because there is a little change in both crown settlement and track settlement after thickness reaches 2 m, and maximum track settlement could satisfy control requirements of this project when thickness of 2 m is being adopted. Therefore, it could be concluded that the grouting reinforcement ring of 2 m is optimal.

Based on the above analysis, optimal parameters for the combined presupport technique have been determined. Through the practical application in Xi'an Station of Metro Line 4, as shown in Figure 9, good effects are obtained. Therefore, for tunnels excavated in the loess area, the combined presupport technique of the pipe shed support and grouting reinforcement is very effective in reducing tunnel deformation and control track settlement.

5. Conclusions

Based on the first shallow tunnel passing below an active railway station in the loess area in China, the studies on the tunnel deformation and track settlement are carried out. To guarantee the safe operation of the railway station during underground excavation, safety evaluation of track settlement is performed and remedial measures of the combined presupport of the pipe roof and grouting reinforcement are presented.

The optimal support parameters are investigated as well. The following conclusions were notable:

- (a) Without adopting other reinforcement measures, the maximum track settlement has far exceeded engineering requirements.
- (b) The installation of the pipe roof support plays an important role in controlling tunnel crown settlement and track settlement. The optimal pipe diameter is 159 mm, and the optimal arrangement area of the pipe roof is 150° .
- (c) Grouting could improve soil strength and reduce deformations. The optimal thickness of the grouting reinforcement ring is 2 m.

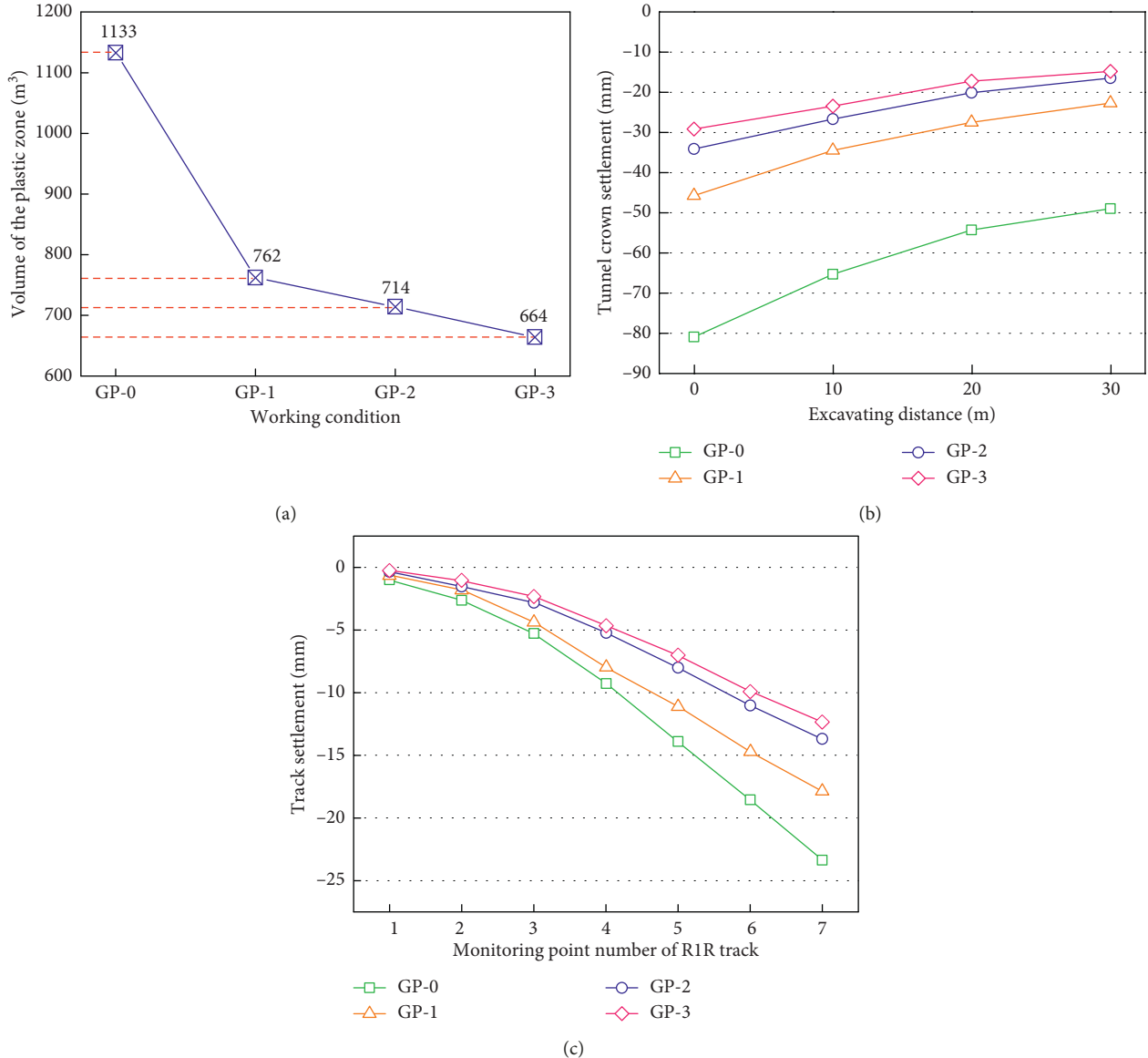


FIGURE 8: (a) Volume of the plastic zone. (b) Tunnel crown settlement. (c) Track settlement with different reinforcement ring thicknesses.



FIGURE 9: Field tests in Xi'an Station of Metro Line 4.

Data Availability

The data used to support the findings of this study are available from the corresponding author upon request.

Conflicts of Interest

The authors declare that they have no conflicts of interest.

Acknowledgments

This work was supported by the National Natural Science Foundation of China (No. 10772143) and the Fund of Shaanxi Science & Technology Co-ordination & Innovation Project (No. 2015TZC-G-8-9).

References

- [1] S. G. Ercelebi, H. Copur, and I. Ocak, "Surface settlement predictions for Istanbul Metro tunnels excavated by EPB-TBM," *Environmental Earth Sciences*, vol. 62, no. 2, pp. 357–365, 2010.
- [2] H. Chakeri, Y. Ozcelik, and B. Unver, "Effects of important factors on surface settlement prediction for metro tunnel excavated by EPB," *Tunnelling and Underground Space Technology*, vol. 36, pp. 14–23, 2013.
- [3] A. Bobet, "Analytical solutions for shallow tunnels in saturated ground," *Journal of Engineering Mechanics*, vol. 127, no. 12, pp. 1258–1266, 2001.
- [4] J. L. Qiu, H. Q. Liu, J. X. Lai, H. Lai, J. Chen, and K. Wang, "Investigating the long term settlement of a tunnel built over improved loessial foundation soil using jet grouting technique," *Journal of Performance of Constructed Facilities*, vol. 32, no. 5, article 04018066, 2018.
- [5] Y. Mahmutoglu, "Surface subsidence induced by twin subway tunnelling in soft ground conditions in Istanbul," *Bulletin of Engineering Geology and the Environment*, vol. 70, no. 1, pp. 115–131, 2011.
- [6] G. P. Lignola, A. Flora, and G. Manfredi, "Simple method for the design of jet grouted umbrellas in tunneling," *Journal of Geotechnical and Geoenvironmental Engineering*, vol. 134, no. 12, pp. 1778–1790, 2008.
- [7] A. H. Høien and B. Nilsen, "Rock mass grouting in the Løren Tunnel: case study with the main focus on the groutability and feasibility of drill parameter interpretation," *Rock Mechanics and Rock Engineering*, vol. 47, no. 3, pp. 967–983, 2014.
- [8] Z. Zhang, H. Li, H. Liu, G. Li, and X. Shi, "Load transferring mechanism of pipe umbrella support in shallow-buried tunnels," *Tunnelling and Underground Space Technology*, vol. 43, pp. 213–221, 2014.
- [9] C. Yoo, "Finite-element analysis of tunnel face reinforced by longitudinal pipes," *Computers and Geotechnics*, vol. 29, no. 1, pp. 73–94, 2002.
- [10] C. S. Wu and Z. D. Zhu, "Analytical method for evaluating the ground surface settlement caused by tail void grouting pressure in shield tunnel construction," *Advances in Civil Engineering*, vol. 2018, Article ID 3729143, 10 pages, 2018.
- [11] H. Park, O. H., Ju-Young, D. Kim, and S. Chang, "Monitoring and analysis of ground settlement induced by tunnelling with slurry pressure-balanced tunnel boring machine," *Advances in Civil Engineering*, vol. 2018, Article ID 5879402, 10 pages, 2018.
- [12] R. Hasanzadeh, H. Chakeri, Y. Ozcelik, and H. Denek, "Evaluation of surface settlements in the Istanbul metro in terms of analytical, numerical and direct measurements," *Bulletin of Engineering Geology and the Environment*, vol. 71, no. 3, pp. 499–510, 2012.
- [13] H. T. Yu, Y. Yuan, G. X. Yu, and X. Liu, "Evaluation of influence of vibrations generated by blasting construction on an existing tunnel in soft soils," *Tunnelling and Underground Space Technology*, vol. 43, pp. 59–66, 2014.
- [14] X. Liu, Y. Liu, Z. Yang, and C. He, "Numerical analysis on the mechanical performance of supporting structures and ground settlement characteristics in construction process of subway station built by pile-beam-arch method," *KSCE Journal of Civil Engineering*, vol. 21, no. 5, pp. 1690–1705, 2016.
- [15] M. H. Sadaghiani and S. Dadizadeh, "Study on the effect of a new construction method for a large span metro underground station in Tabriz-Iran," *Tunnelling and Underground Space Technology*, vol. 25, no. 1, pp. 63–69, 2010.
- [16] V. A. Kivi, M. H. Sadaghiani, and M. M. Ahmadi, "Numerical modeling of ground settlement control of large span underground metro station in Tehran Metro using Central Beam Column (CBC) structure," *Tunnelling and Underground Space Technology*, vol. 28, no. 1, pp. 1–9, 2012.
- [17] Y. Zhao, H. He, and P. Li, "Key techniques for the construction of high-speed railway large-section loess tunnels," *Engineering*, vol. 4, no. 2, pp. 254–259, 2018.
- [18] P. F. Li, Y. Zhao, and X. J. Zhou, "Displacement characteristics of high-speed railway tunnel construction in loess ground by using multi-step excavation method," *Tunnelling and Underground Space Technology*, vol. 51, pp. 41–55, 2016.
- [19] J. Qiu, Y. Qin, J. Lai et al., "Structural response of the metro tunnel under local dynamic water environment in loess strata," *Geofluids*, vol. 2019, Article ID 8541959, 16 pages, 2019.
- [20] W. Kui, Z. Qinwen, S. Zhushan, and Z. Zhenlong, "Research into the effect of different tunnel excavation methods on rail track settlement," *Indian Geotechnical Journal*, pp. 1–9, 2018.

